Electronic Supplementary Information (ESI)

Poly(dibenzothiophenylene sulfide)s: Sulfur-rich Annulated Frameworks with Wide-range Ultrahigh Refractive Index

Seigo Watanabe,[a] Zexin An,[b] Hiromichi Nishio,[b] Yoshino Tsunekawa,[b] and Kenichi Oyaizu*[a,b]

a. Research Institute for Science and Engineering, Waseda University, 3-4-1 Okubo, Shinjuku-ku, Tokyo 169-8555, Japan.
b. Department of Applied Chemistry, Waseda University, 3-4-1 Okubo, Shinjuku-ku, Tokyo 169-8555, Japan

E-mail: oyaizu@waseda.jp

1. Additional experimental information

1.1. Materials

2-Bromodibenzothiphene, iodine, trifluoroacetic acid (TFA), 1,2-ethanedithiol, 2,3-dichloro-5,6-dicyano-1,4-benzoquionone (DDQ), and boron tribromide (BBr_3) were purchased from Tokyo Chemical Industry Co. Copper sulfate pentahydrate, potassium hydroxide, N,N-dimethylformamide (DMF), dimethyl sulfoxide (DMSO), hydrochloric acid, hexane, 1,2-dichloroethane (DCE), 1,1,2,2-tetrachloroethane, sodium chloride, sodium hydroxide, and sodium sulfate were purchased from Kanto Chemical Co. Ethyl acetate and chloroform were purchased from Junsei Chemical Co. Methanol and acetone were purchased from Kokusan Chemical Co.

1.2. Synthesis of dibenzothiophene-2-thiol

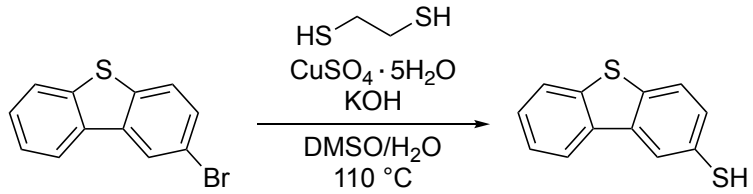

Scheme S1

The following protocol was designed according to the previous report.[1] To a 50 mL flask were added 2-bromodibenzothiophene (3.00 g, 11.4 mmol), copper(II) sulfate pentahydrate (0.14 g, 0.57 mmol), and potassium hydroxide (3.20 g, 57.0 mmol), were dissolved in DMSO/water (= 1/10 (v/v)) mixture (25.1 mL), was subsequently added 1,2-ethanedithiol (2.05 mL, 22.8 mmol), and the solution was stirred at 110 °C for 20 hours. After quenching the solution with 5 vol% hydrochloric acid, the solution was extracted with ethyl acetate, was washed with water and brine, was dehydrated by sodium sulfate. The crude product was purified with column chromatography (hexane/chloroform (= 6/1 (v/v))) to obtain dibenzothiophene-2-thiol as a yellow solid (0.91 g, yield: 36 %). The ^{1}H and ^{13}C NMR spectra have been displayed as Fig. S1 and S2, respectively (While several unassignable signals were observed, they have completely disappeared in the spectra of purified **DBTDPS**: vide infra). FAB-MS (*m*/*z*): $C_{12}H_8S_2$, $[M]^+$ calcd, 216.0; found, 215.9.

1.3. Synthesis of bis(2-dibenzothiophenyl) disulfide (DBTDPS)

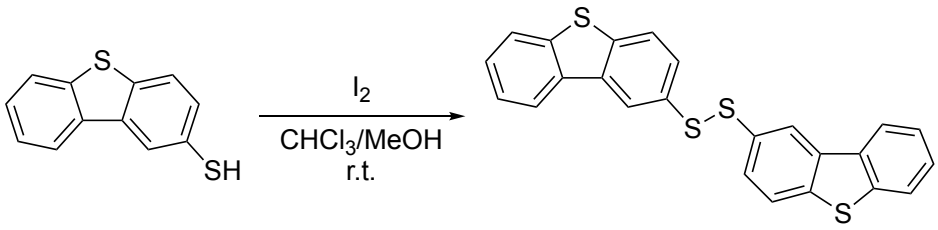

Scheme S2

The protocol was based on our previous report.[2] To a 200 mL beaker was dissolved dibenzothiophene-2-thiol (1.00 g, 4.67 mmol) in chloroform (60 mL) at room temperature. Subsequently, iodine (0.59 g, 2.34 mmol) in methanol (8 mL) was added and was stirred for 1 hour. The solution was extracted with chloroform, was washed with 5 vol% hydrochloric acid, 10 wt% sodium hydroxide

aqueous, and brine, and was dehydrated with sodium sulfate. After removing the solvent with a rotary evaporator, the crude product was recrystallized with chloroform/methanol (= 1/10 (v/v)) to give bis(2-dibenzothiophenyl) disulfide (**DBTDPS**) as a yellow crystal (0.74 g, yield: 75 %). The ^{1}H, ^{13}C, and ^{13}C DEPT NMR spectra have been displayed in Fig. S3, S4, and S5, respectively. FAB-MS (*m*/*z*): $C_{24}H_{14}S_4$, $[M]^+$ calcd, 430.0; found, 429.3.

1.4. Computational calculation

The density functional theory (DFT) calculation was conducted by Gaussian 16 software[3] installed in the computer of our laboratory (intel Corei9). Following our previous report,[4] the geometries of compounds were optimized under ωB97XD/6-31G(d,p) level of theory.

2. Additional figures

2.1. Monomer synthesis

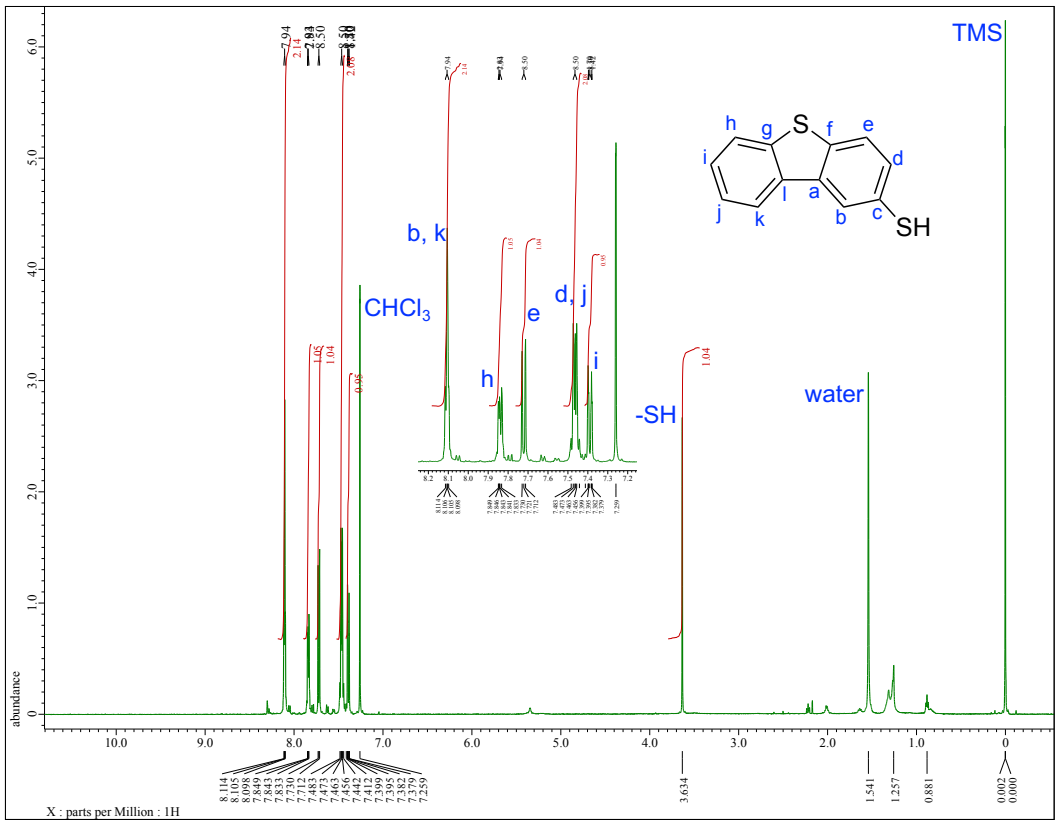

Fig. S1. ^{1}H NMR spectrum of the intermediate (dibenzothiophene-2-thiol) in chloroform-*d* (inset: expanded spectrum for the aromatic region).

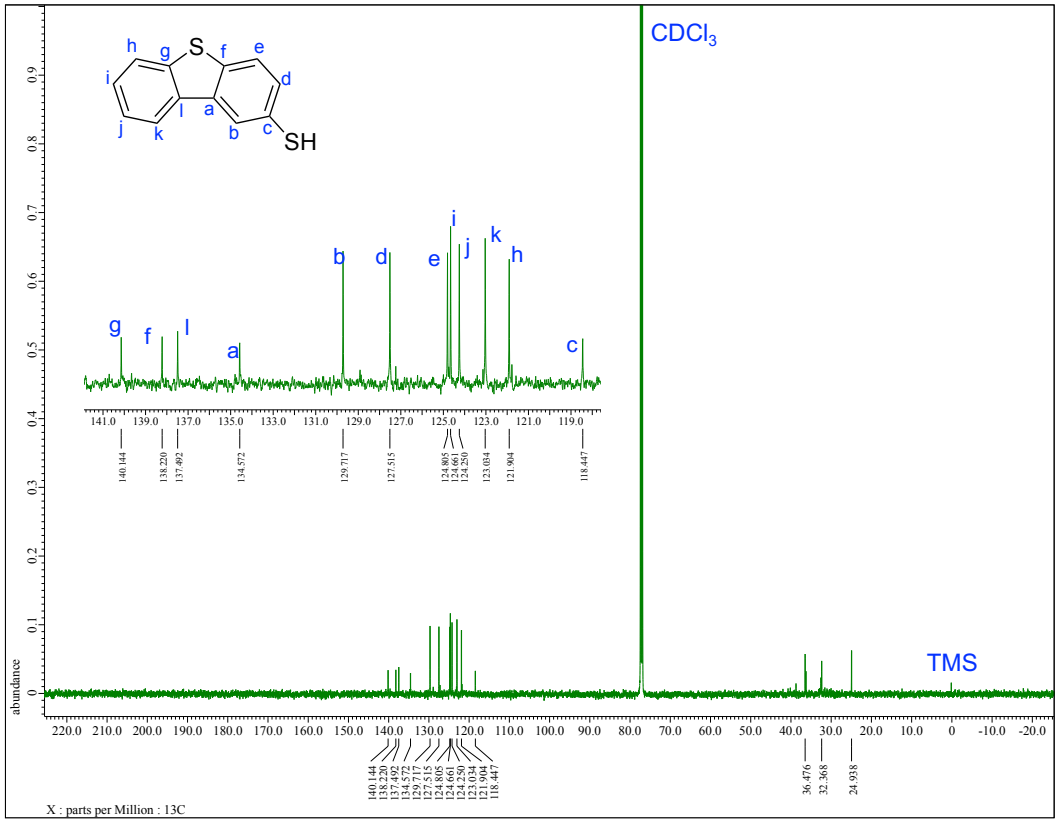

Fig. S2. ^{13}C NMR spectrum of the intermediate (dibenzothiophene-2-thiol) in chloroform-*d* (inset: expanded spectrum for the aromatic region).

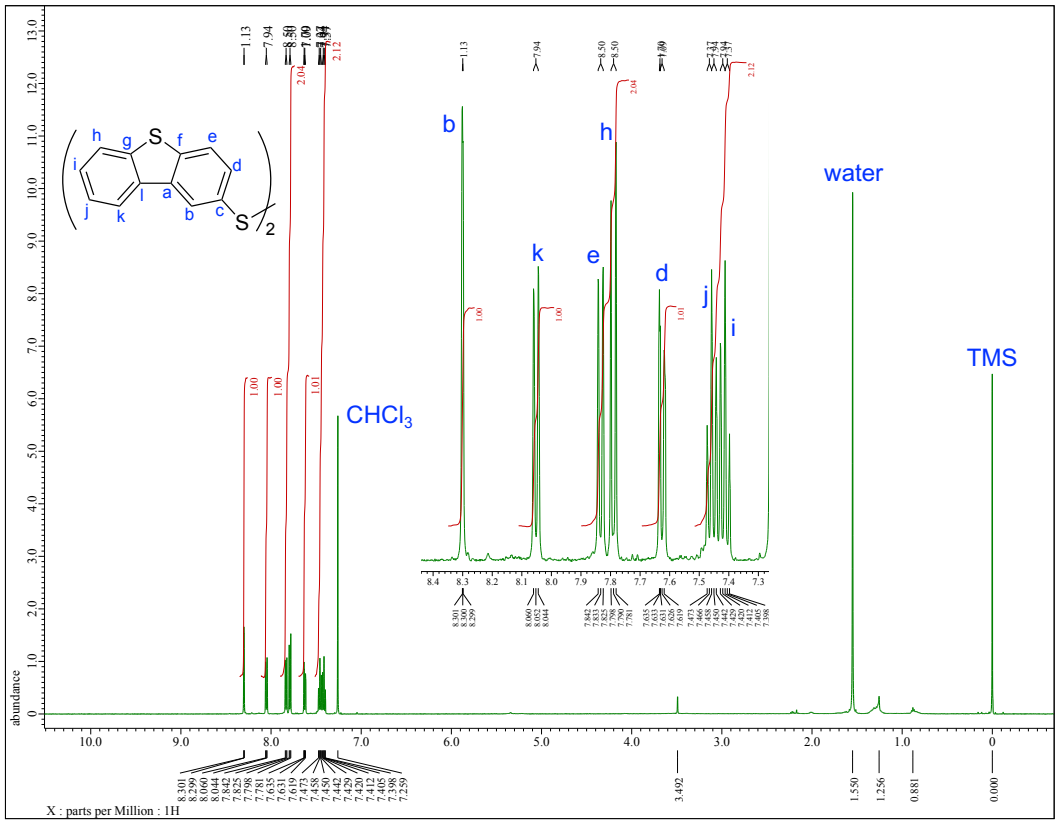

Fig. S3. ^{1}H NMR spectrum of **DBTDPS** in chloroform-*d* (inset: expanded spectrum for the aromatic region).

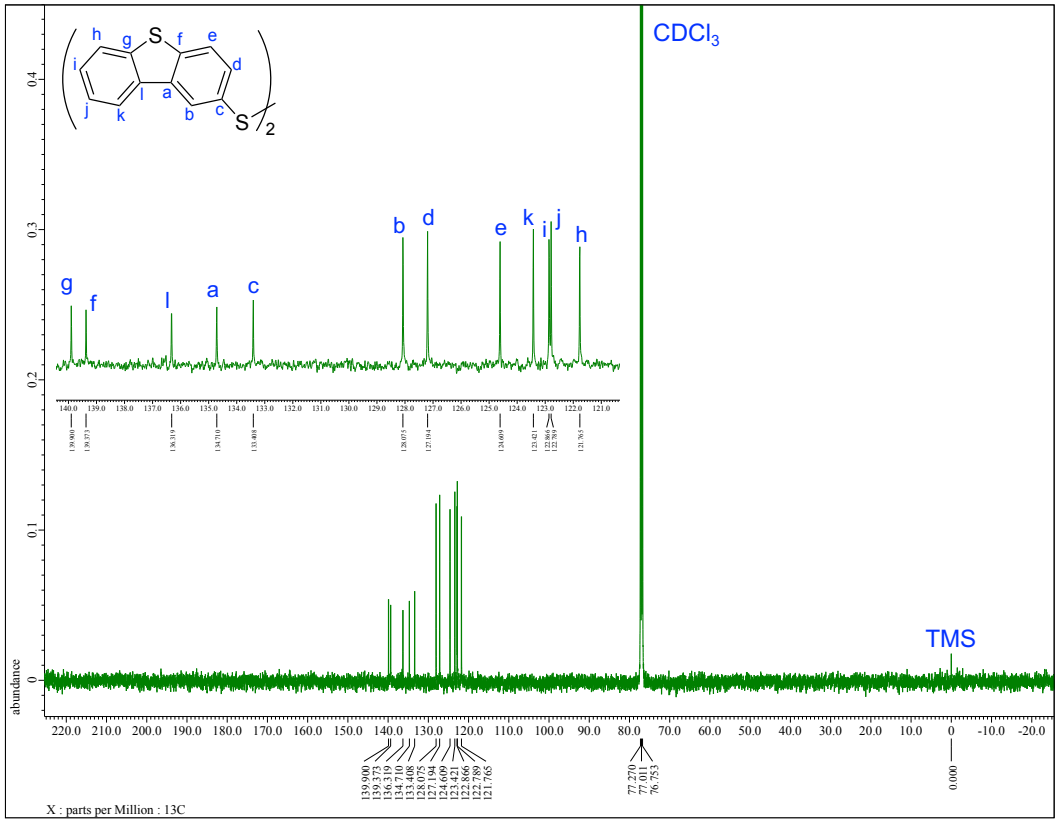

Fig. S4. ^{13}C NMR spectrum of **DBTDPS** in chloroform-*d* (inset: expanded spectrum for the aromatic region).

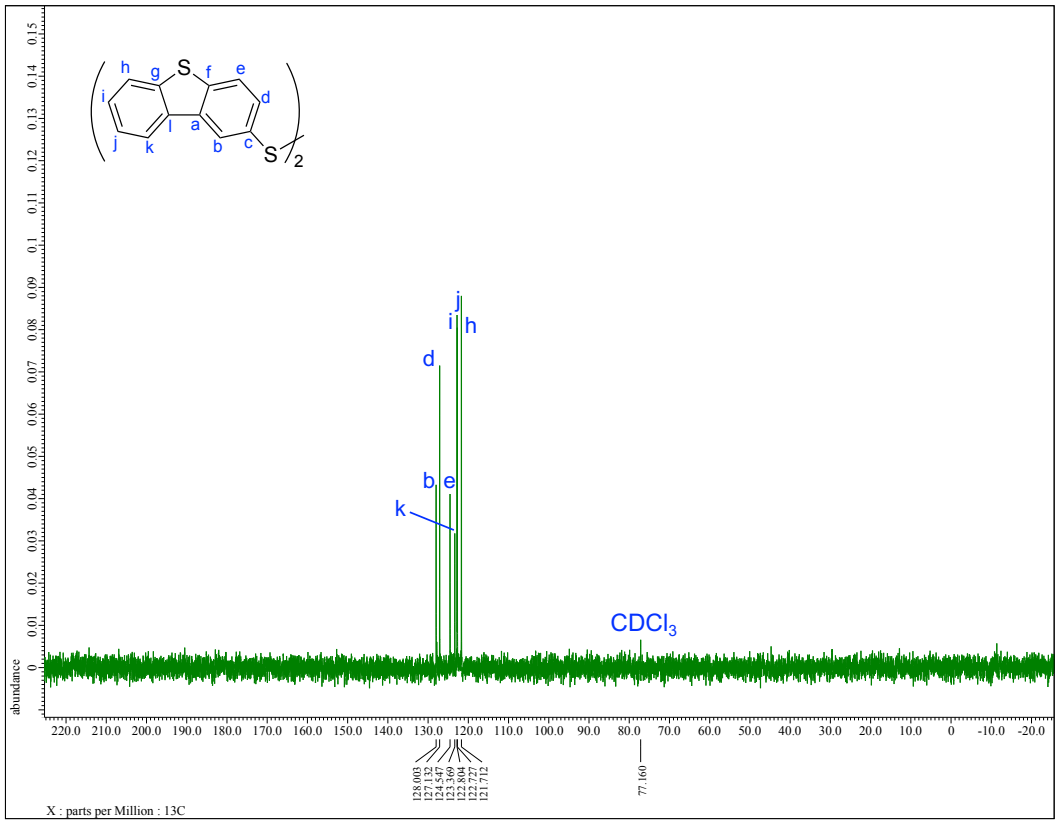

Fig. S5. ^{13}C DEPT NMR spectrum of **DBTDPS** in chloroform-*d*.

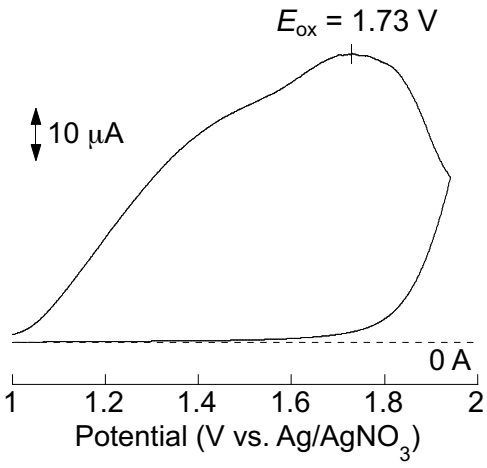

Fig. S6. Cyclic voltammogram of **DBTDPS** in DCM solution (10 mM) containing 0.1 M $TBABF_4$ (scan rate: 0.1 V s^{-1}).

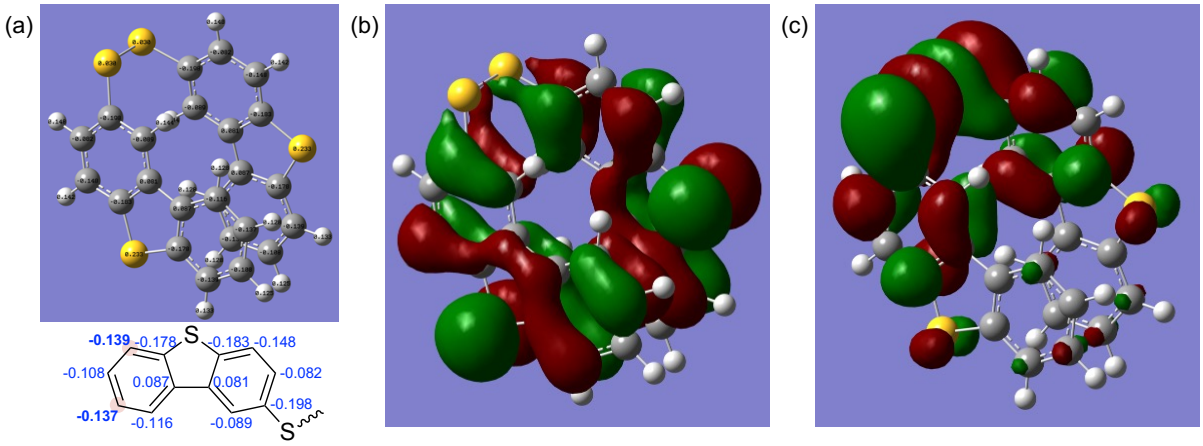

Fig. S7. Results of the DFT calculation for the monomer (**DBTDPS**). Calculation conditions are summarized in the experimental section. (a) Mulliken charge distribution. (b) HOMO. (c) LUMO.

2.2. Synthesis of poly(dibenzothiophenylene sulfide) (PDBTS)

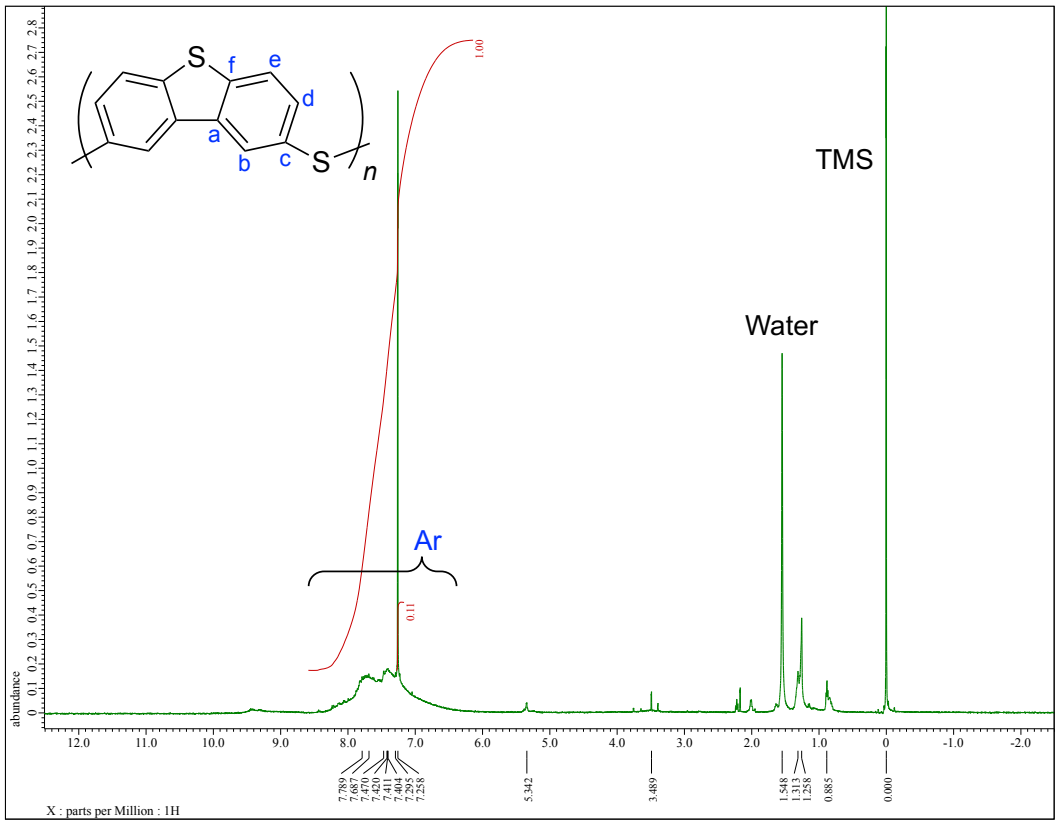

Fig. S8. ^{1}H NMR spectrum of **PDBTS** in chloroform-*d*.

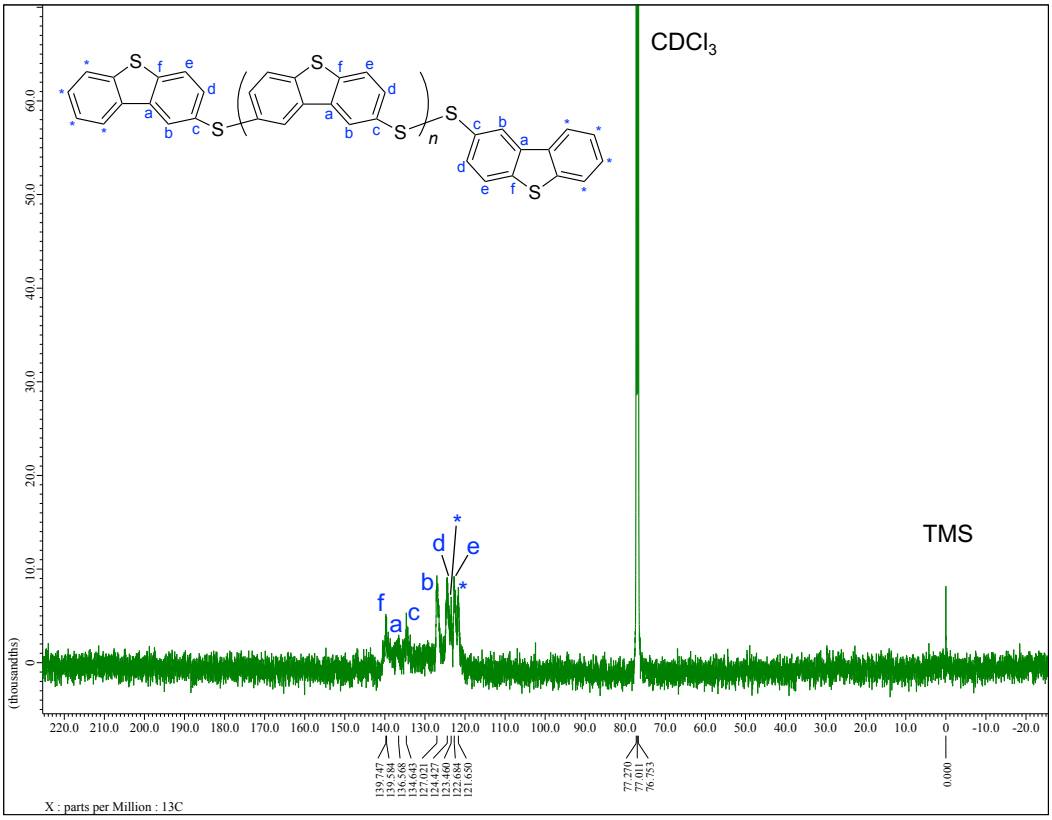

Fig. S9. ^{13}C NMR spectrum of **PDBTS** in chloroform-*d* (*: terminal aromatic carbons).

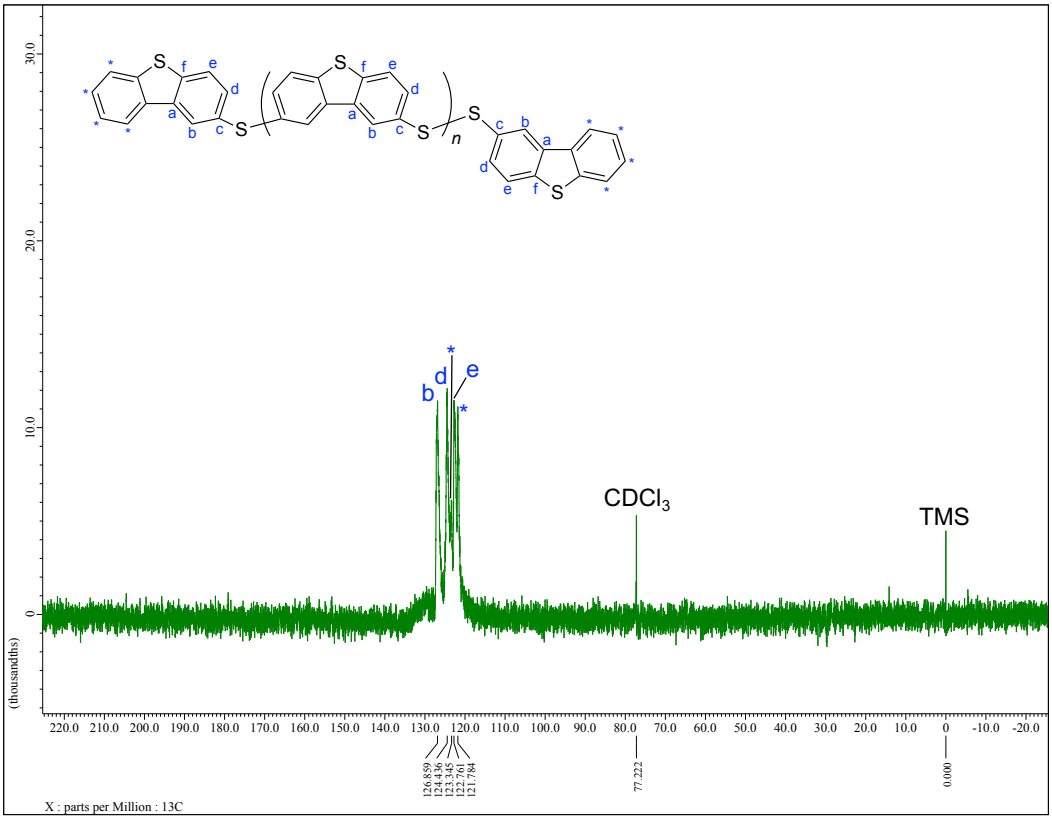

Fig. S10. ^{13}C DEPT spectrum of **PDBTS** in chloroform-*d* (*: terminal aromatic carbons).

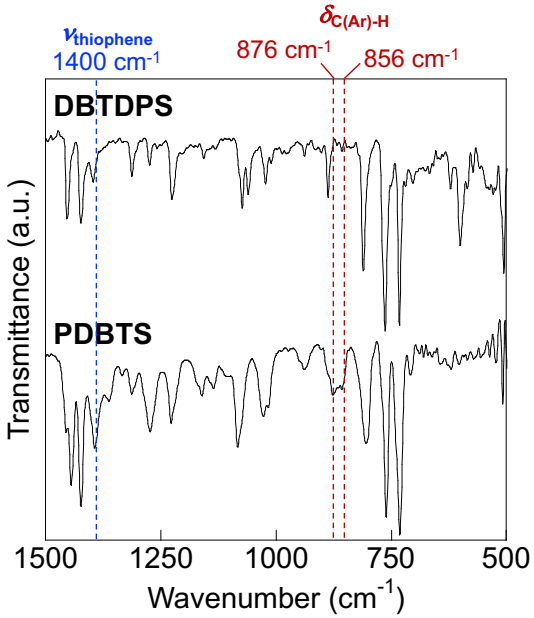

Fig. S11. IR spectra of **DBTDPS** and **PDBTS**.

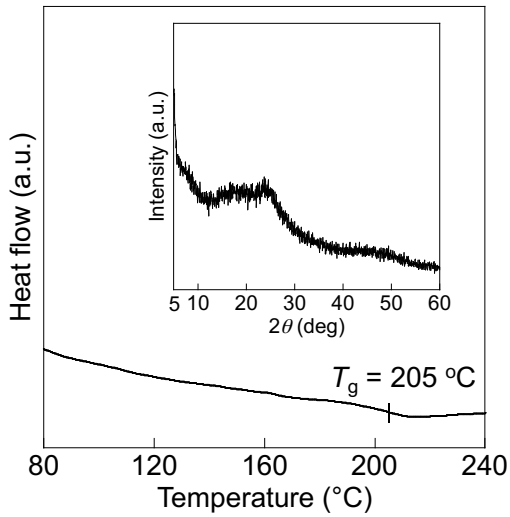

Fig. S12. DSC thermogram of **PDBTS** (inset: powder XRD profile of **PDBTS**).

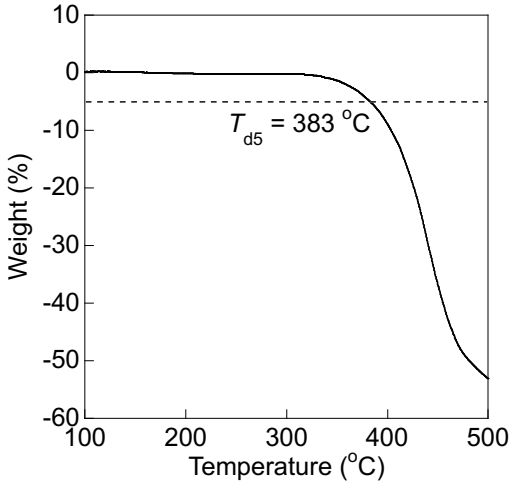

Fig. S13. TGA trace of **PDBTS** (dotted line: 5 % degradation).

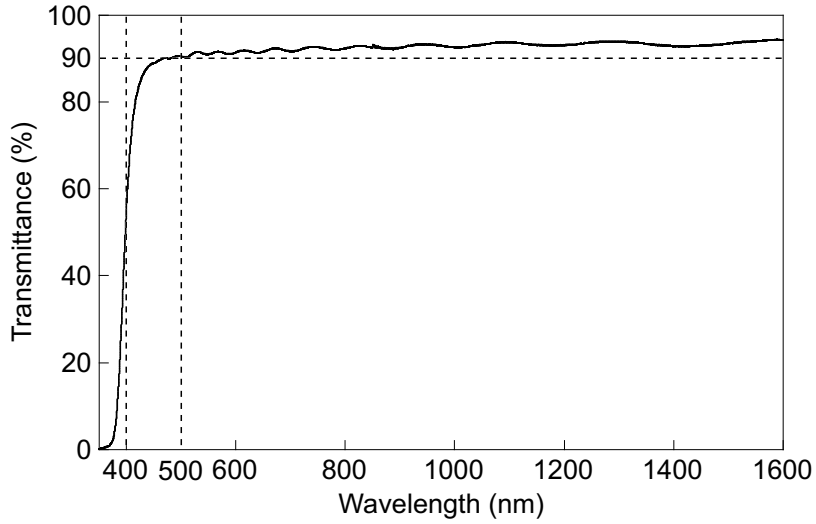

Fig. S14. Original UV-vis spectrum of the **PDBTS** film (thickness: 3.0 μm).

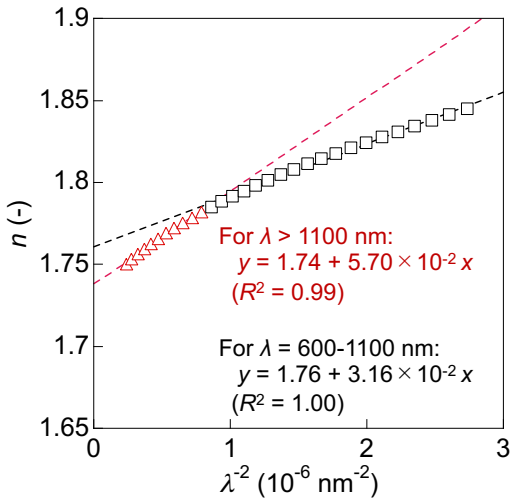

Fig. S15. RI-λ^{-2} plots for the **PDBTS** film. The raw data belongs to the RI spectra obtained by the ellipsometry. Note that the plots are composed of the data from short (600-1100 nm, black) and long (over 1100 nm, red) wavelength regions for fitting precisely.

2.3. Synthesis of copolymers vis oxidative polymerization (CP1 and CP2)

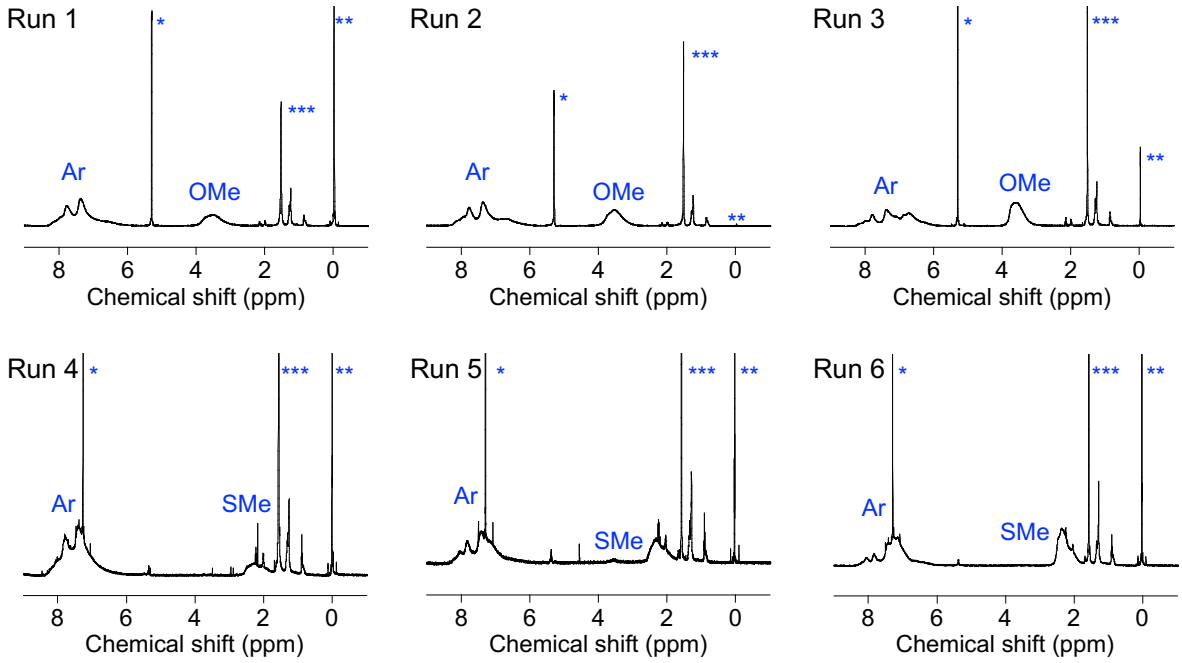

Fig. S16. ^{1}H NMR spectra of **CP1** and **CP2** in dichloromethane-d_2 (run 1-3) or chloroform-d (run 4-6). *: CH_2Cl_2 or $CHCl_3$, **: TMS, and ***: water.

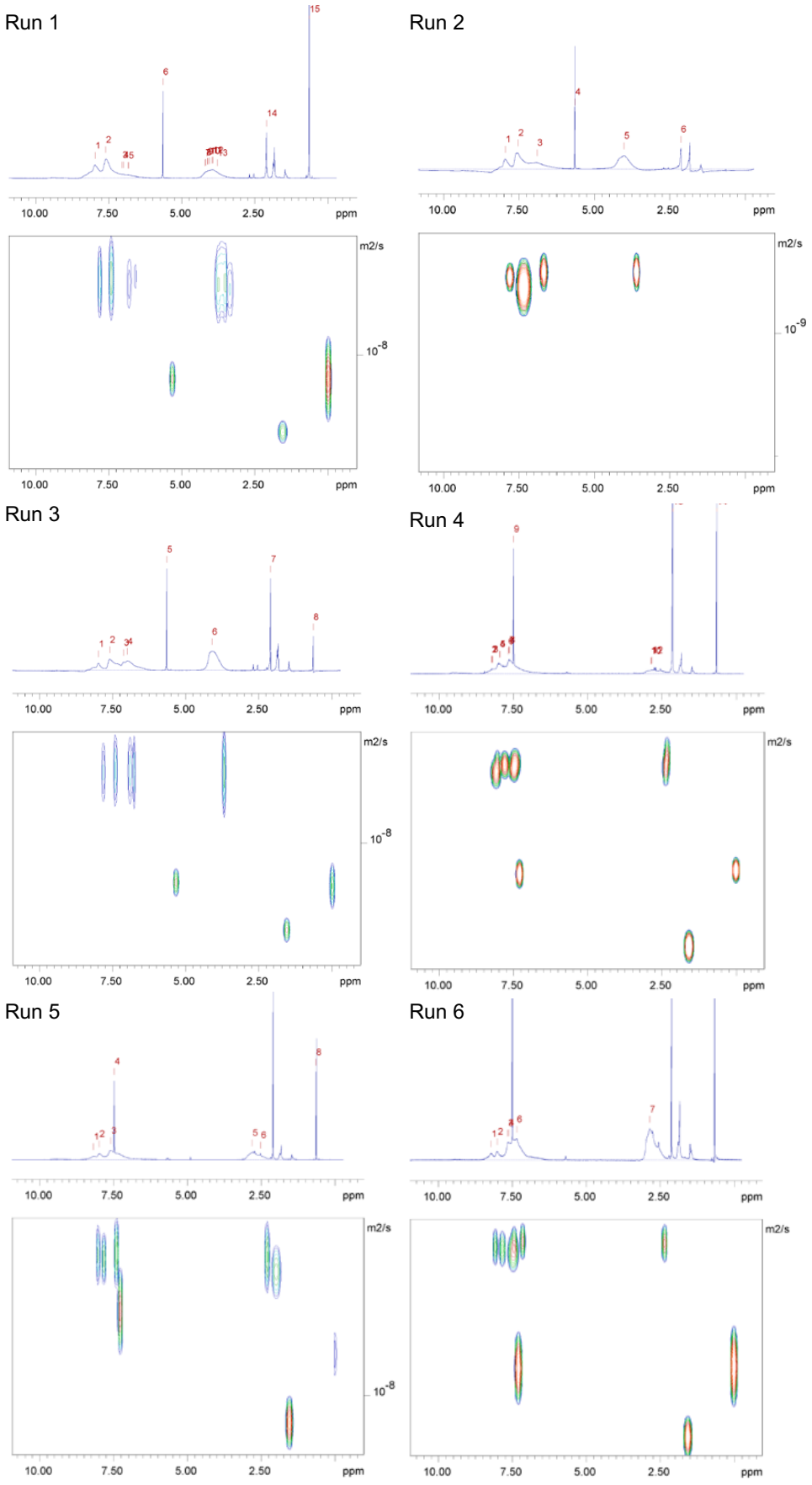

Fig. S17. DOSY-NMR spectra of **CP1** and **CP2** in dichloromethane-d_2 (run 1-3) or chloroform-*d* (run 4-6).

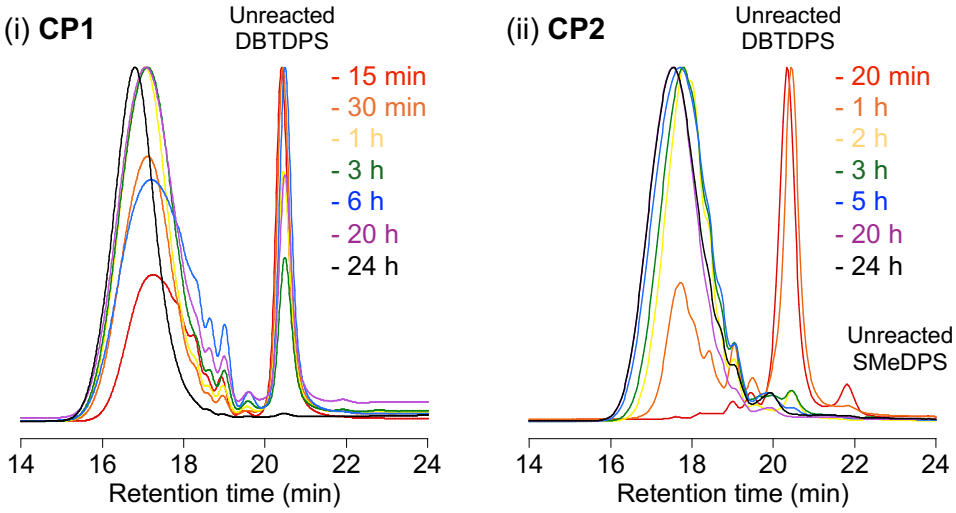

Fig. S18. Time-course SEC chromatograms (eluent: chloroform) for the oxidative polymerization of (i) [**DBTDPS**]/[**OMeDPS**] = 1/1 or (ii) [**DBTDPS**]/[**SMeDPS**] = 1/1.

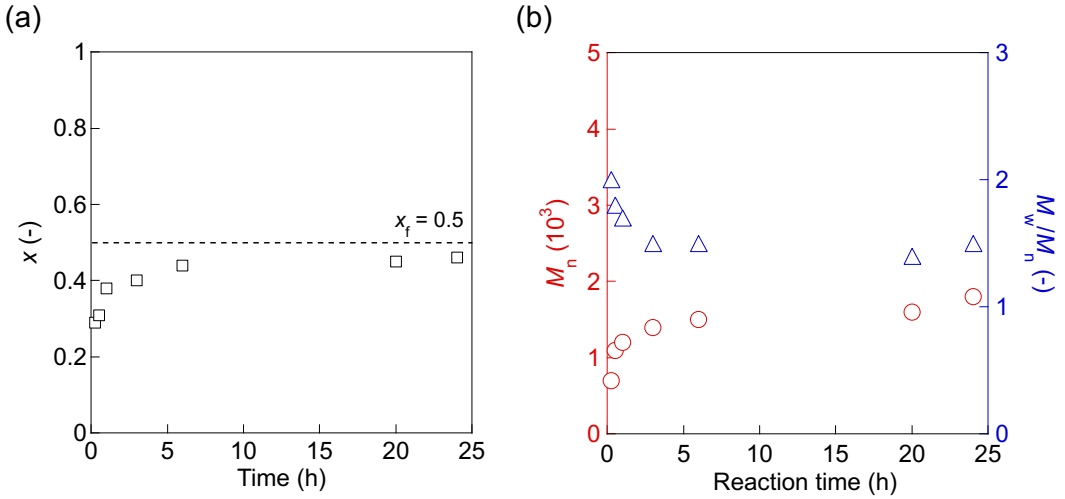

Fig. S19. Time-course molecular weight for the oxidative polymerization of [**DBTDPS**]/[**OMeDPS**] = 1/1: (a) x. (b) M_n (red circles) and M_w/M_n (blue triangles). The raw chromatograms correspond to Fig. S18(i).

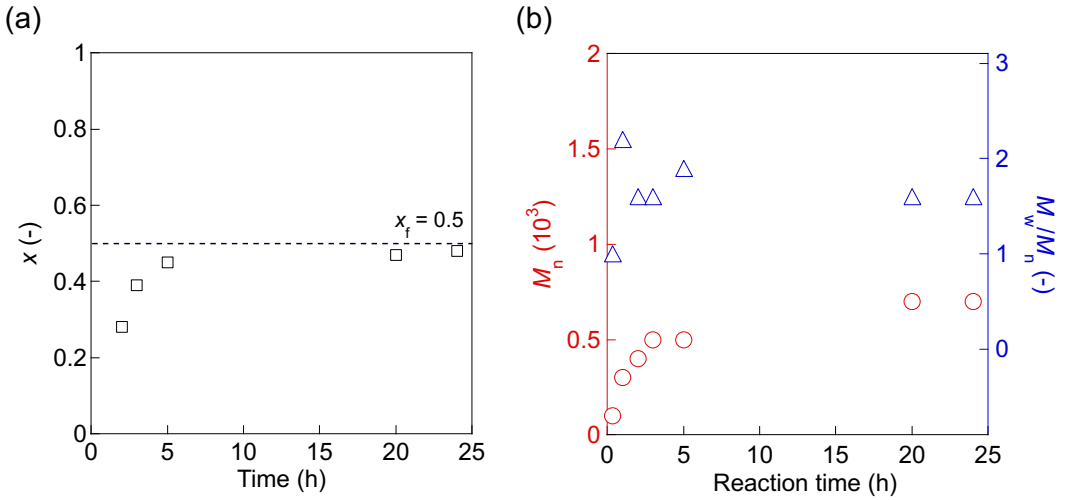

Fig. S20. Time-course molecular weight for the oxidative polymerization of [**DBTDPS**]/[**SMeDPS**] = 1/1: (a) x. (b) M_n (red circles) and M_w/M_n (blue triangles). The raw chromatograms correspond to Fig. S18(ii). Note that the x values at 20 min and 1 h were not determined due to the trace amount of fractions unable to perform the ^{1}H NMR measurements.

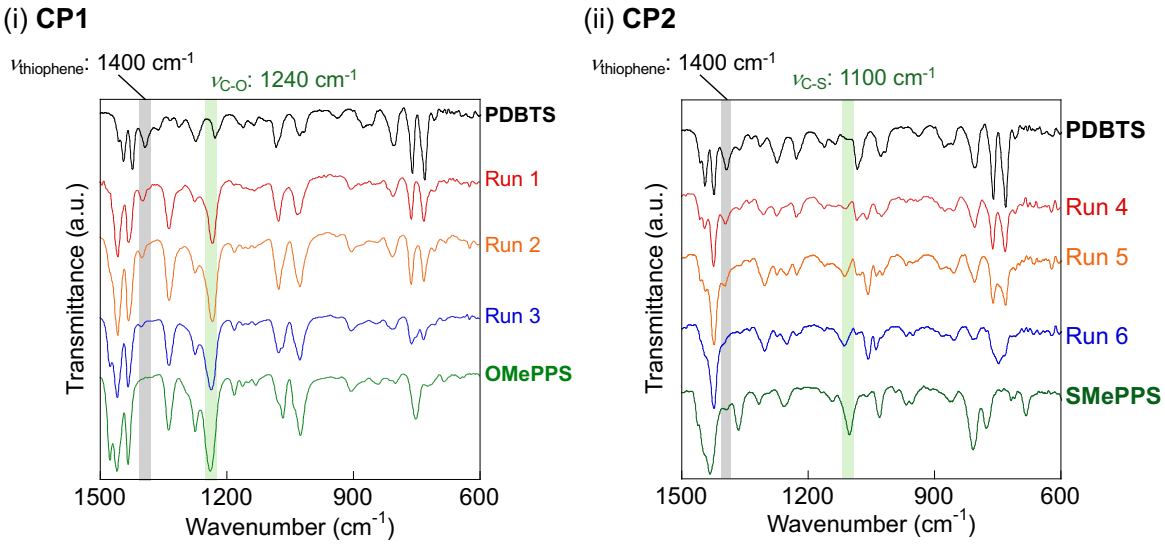

Fig. S21. IR spectra of (i) **CP1** and (ii) **CP2**, including the spectra of the corresponding homopolymers.

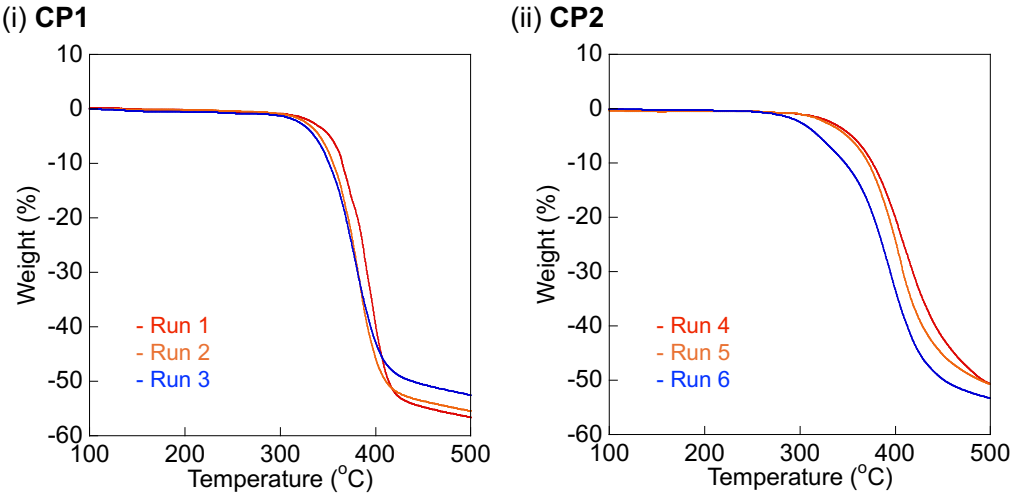

Fig. S22. TGA traces of (i) **CP1** and (ii) **CP2**.

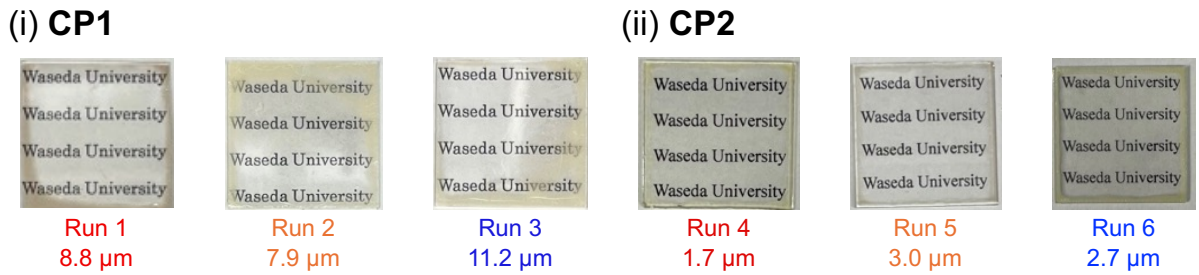

Fig. S23. Thin films (including their thickness) of (i) **CP1** and (ii) **CP2** on glass substrates.

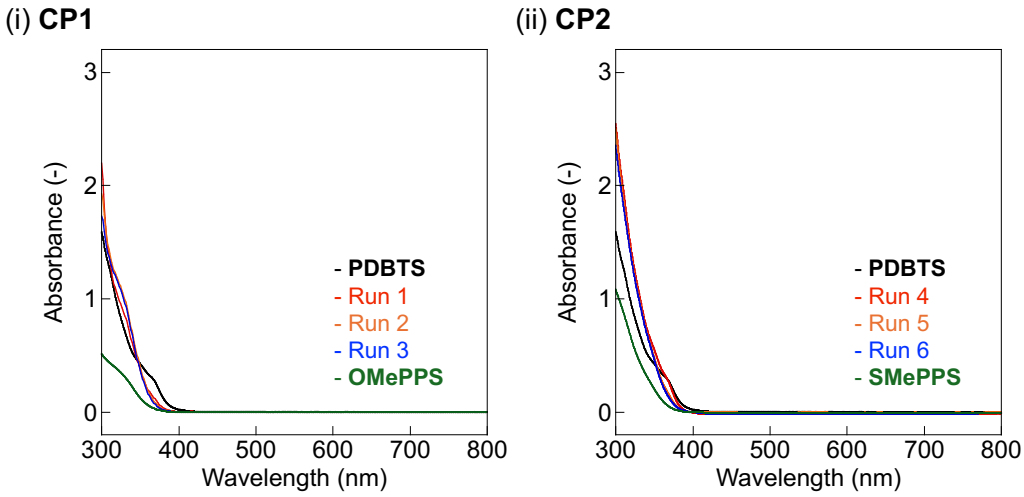

Fig. S24. UV-vis spectra of (i) **CP1** and (ii) **CP2** and the corresponding homopolymers (0.1 mM solution in chloroform). The data of **OMePPS** and **SMePPS** were adopted from our previous reports: supplementary ref. 5 (Copyright © 2020 The Chemical Society of Japan) and ref. 2 (under the CC-BY-NC-ND 4.0 license), respectively.

2.4. Synthesis of hydroxy-containing copolymers (CP3)

Table S1 Synthesis of **CP3**

Run	Feed **CP2**	Yield (%)	Unit ratio x^a (-)	Yield (%)
7	Run 1 (x = 0.65)	83	0.64	49
8	Run 2 (x = 0.46)	86	0.47	53
9	Run 3 (x = 0.25)	91	0.24	49

[a]Determined by ^{1}H NMR.

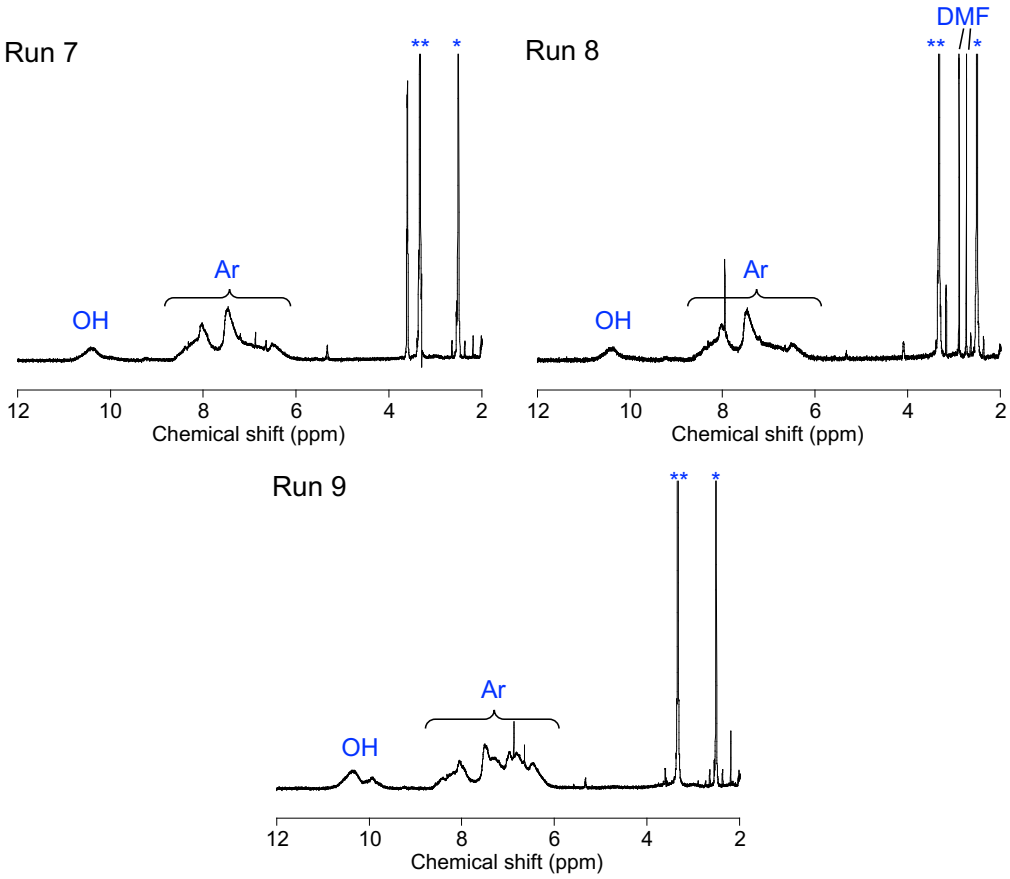

Fig. S25. ^{1}H NMR spectra of **CP3** in DMSO-d_6. The run numbers correspond to those for **Table 2.** *: DMSO **: water.

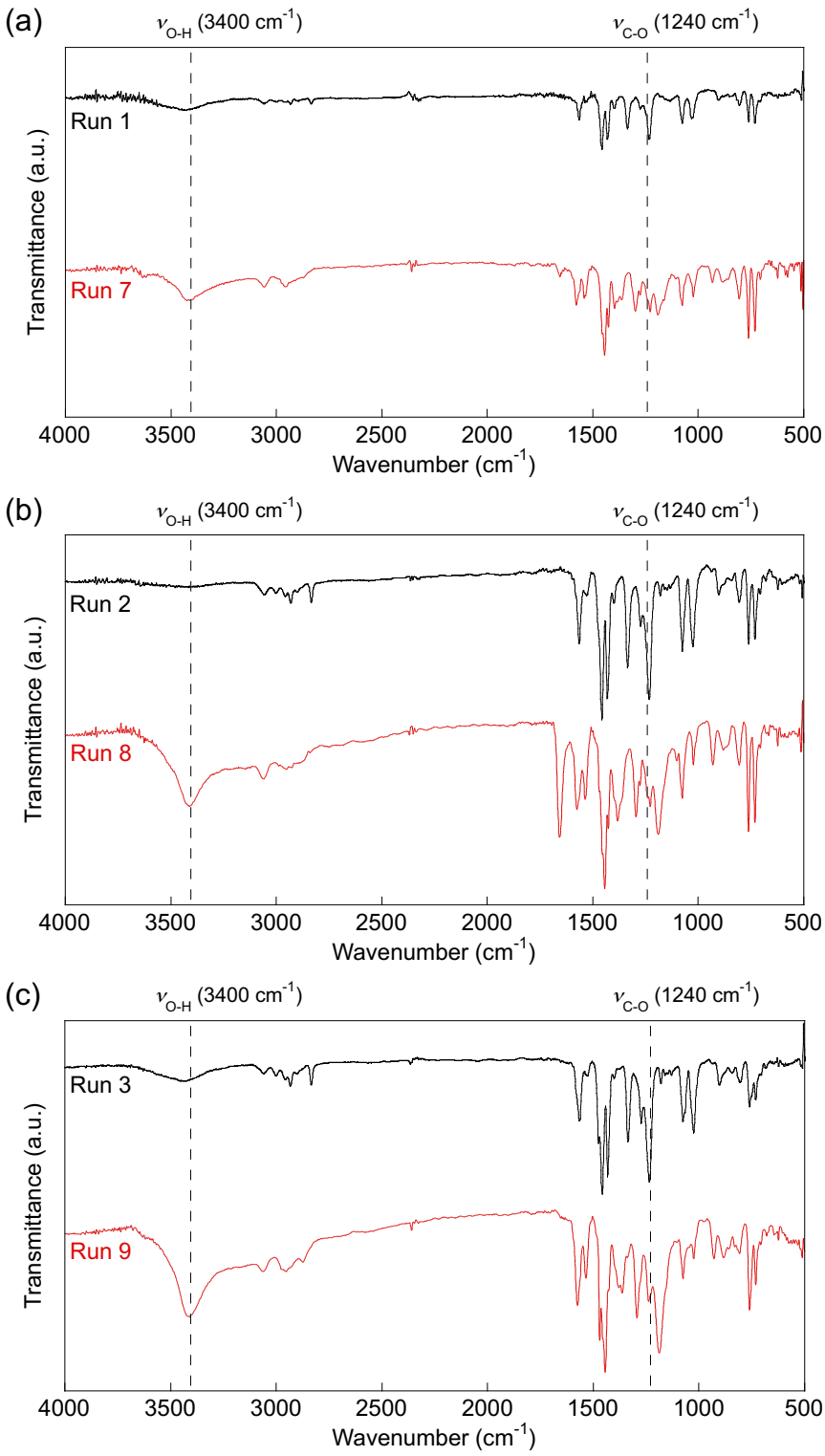

Fig. S26. IR spectra of **CP1** and **CP3** before and after the demethylation: (a) Run 1 and 7, (b) Run 2 and 8, and (c) Run 3 and 9.

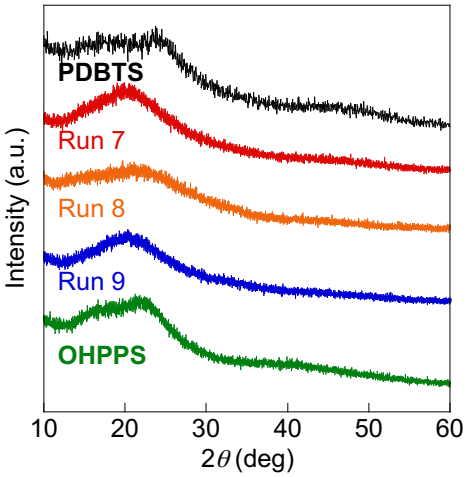

Fig. S27. XRD patterns of **CP3** and the corresponding homopolymers (**PDBTS** and **OHPPS**).

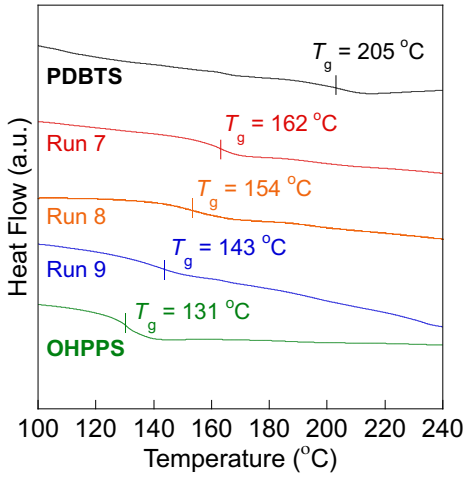

Fig. S28. DSC thermograms of **CP3** and the corresponding homopolymers (2nd heating, scanning rate: 20 °C min^{-1}).

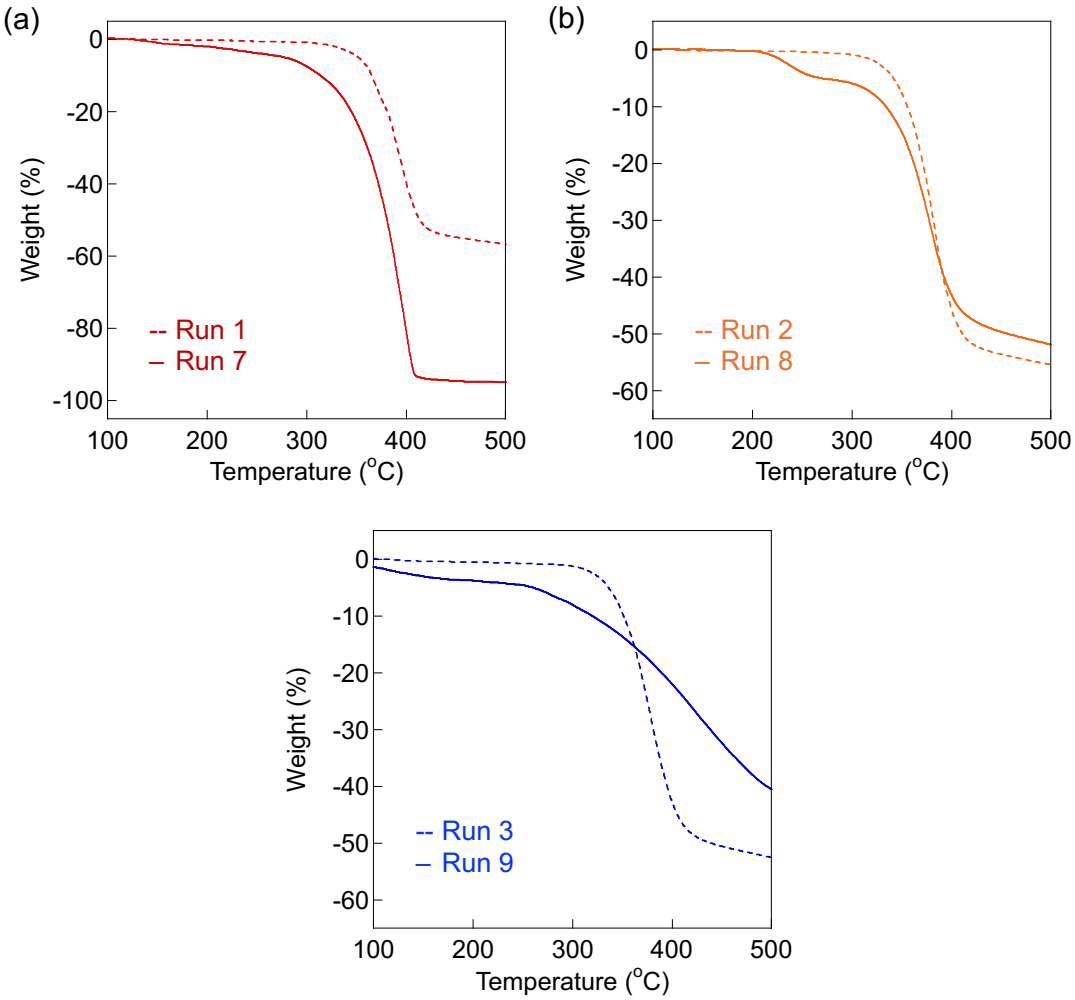

Fig. S29. TGA curves of **CP1** and **CP3** (before and after the demethylation): (a) Run 1 and 7, (b) Run 2 and 8, and (c) Run 3 and 9.

Table S2 Summary of thermal and optical properties of **CP2** and **CP3**

Run	x^a (-)	$T_g{}^b$ (°C)	$T_{d5}{}^c$ (°C)	$\varepsilon_{360}{}^{de}$ (10^3 M^{-1} cm^{-1})	$\%T_{400}{}^{df}$	$n_D{}^g$ (-)	$\nu_D{}^g$ (-)
1	0.65	172	352	2.5	90	1.80	16
7	0.64	162	279	1.7	93	1.79	13
2	0.46	156	342	2.3	93	1.78	18
8	0.47	154	270	1.5	95	1.77	15
3	0.25	147	336	1.7	97	1.76	16
9	0.24	143	260	1.3	96	1.82	12

[a]Determined by ^{1}H NMR. [b]Determined by DSC. [c]Determined by TGA. [d]UV-vis spectroscopy. [e]Values for DMF solution (measured concn.: 0.1 mM). [f]Normalized values with 1 μm thickness. [g]Determined by spectroscopic ellipsometry.

Fig. S30. Thin films (including their thickness) of **CP3** on glass substrates.

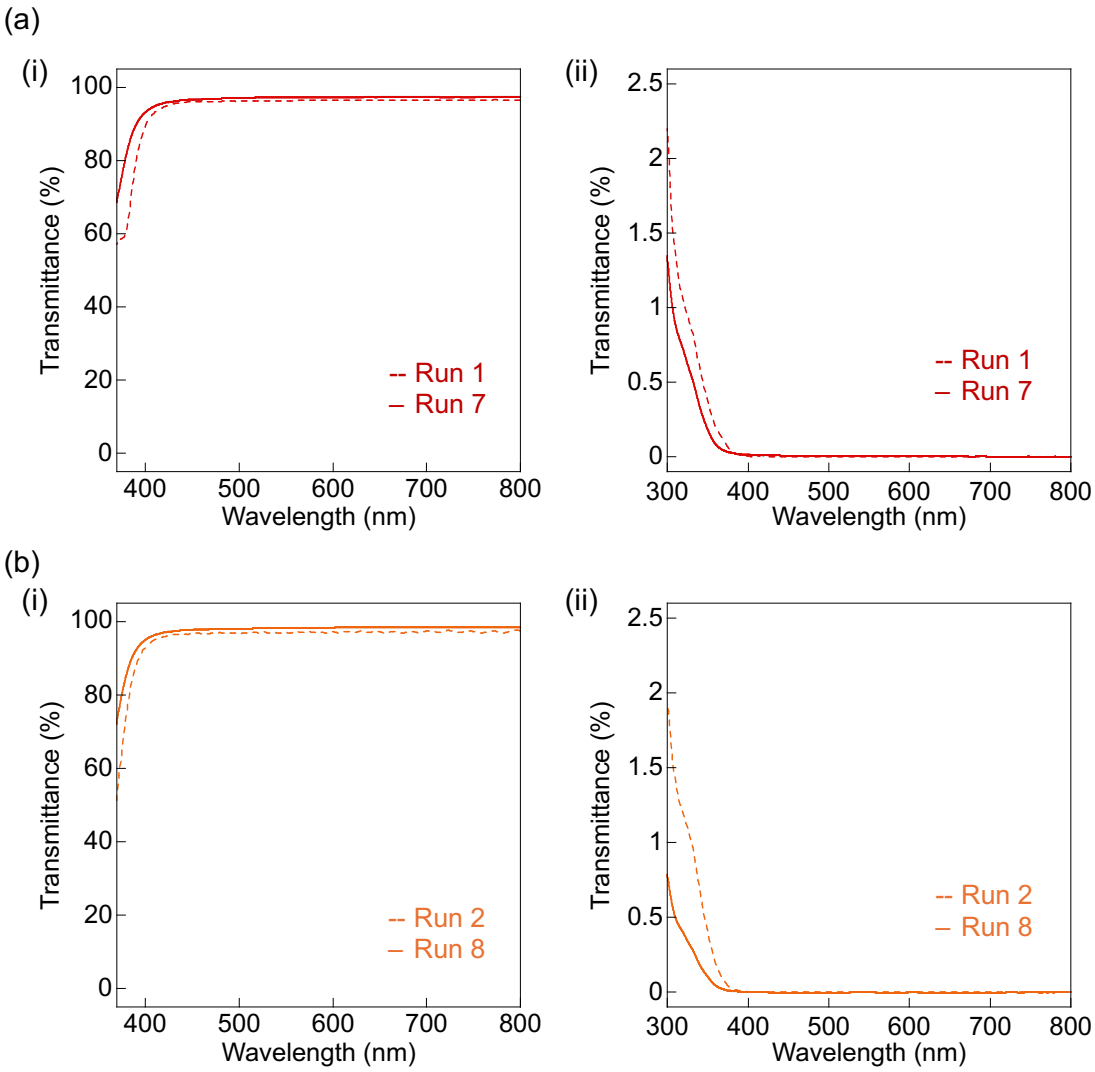

Fig. S31. UV-vis spectra of the (i) films (normalized in 1 μ m thickness) and (ii) solution (0.1 mM in DMF) of **CP1** and **CP3**. Note that the spectra for Run 3 and 9 are displayed as Fig. 6c (i).

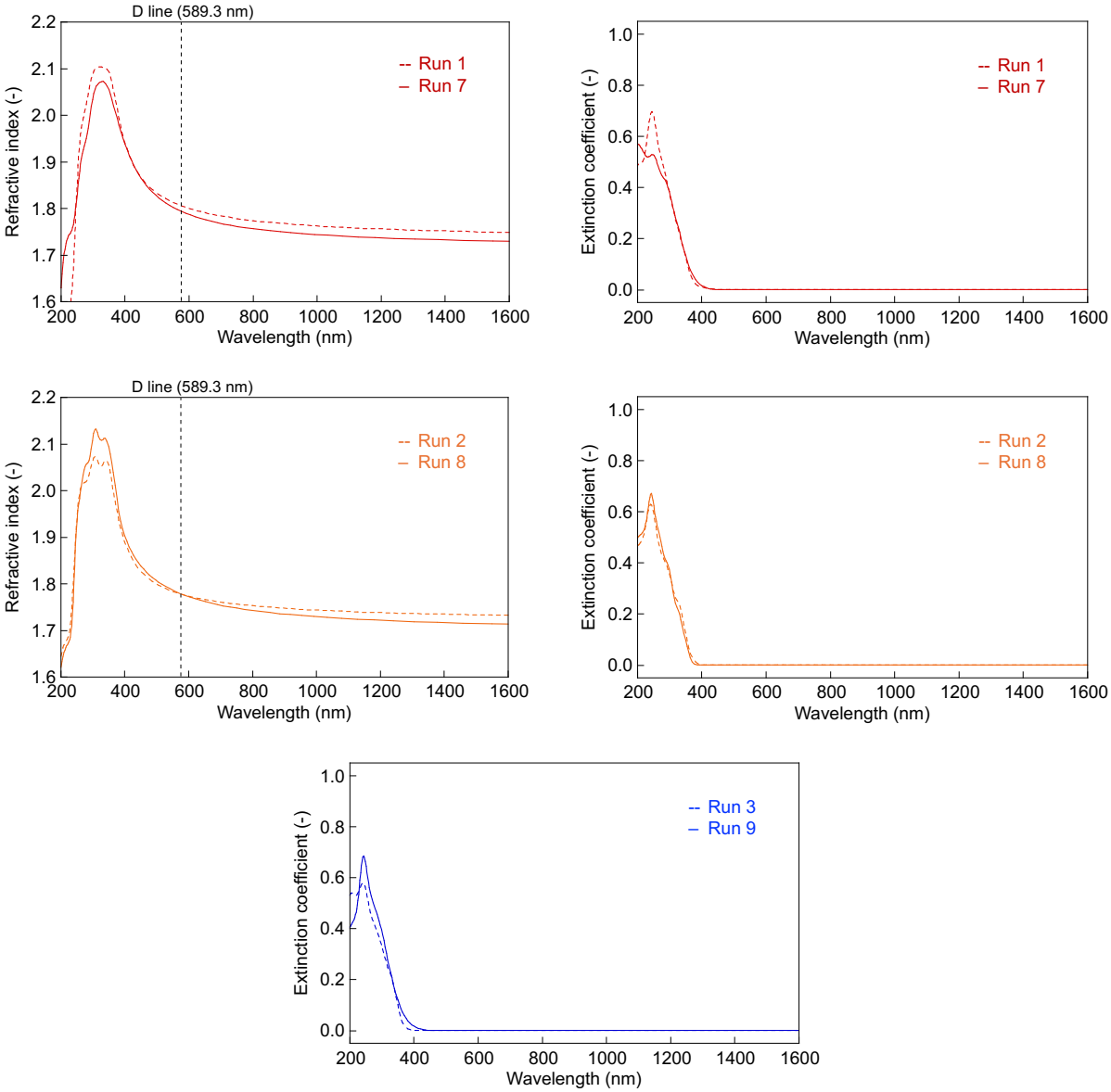

Fig. S32. RI (n) and extinction coefficient (k) of **CP1** and **CP3** in the near UV-visible-NIR range: (top) Run 1 and 7, (middle) Run 2 and 8, (bottom) Run 3 and 9. Note that n spectra for Run 3 and 9 are displayed as Fig. 6c (ii).

Supplementary references

1 Y. Liu, J. Kim, H. Seo, S. Park and J. Chae, *Adv. Synth. Catal.*, 2015, **357**, 2205–2212.

2 S. Watanabe, T. Takayama and K. Oyaizu, *ACS Polym Au*, 2022, **2**, 458–466.

3 M. J. Frisch, G. W. Trucks, H. B. Schlegel, G. E. Scuseria, M. A. Robb, J. R. Cheeseman, G. Scalmani, V. Barone, G. A. Petersson, H. Nakatsuji, X. Li, M. Caricato, A. V. Marenich, J. Bloino, B. G. Janesko, R. Gomperts, B. Mennucci, H. P. Hratchian, J. V. Ortiz, A. F. Izmaylov, J. L. Sonnenberg, D. Williams-Young, F. Ding, F. Lipparini, F. Egidi, J. Goings, B. Peng, A. Petrone, T. Henderson, D. Ranasinghe, V. G. Zakrzewski, J. Gao, N. Rega, G. Zheng, W. Liang, M. Hada, M. Ehara, K. Toyota, R. Fukuda, J. Hasegawa, M. Ishida, T. Nakajima, Y. Honda, O. Kitao, H. Nakai, T. Vreven, K. Throssell, J. A. Montgomery Jr, J. E. Peralta, F. Ogliaro, M. J. Bearpark, J. J. Heyd, E. N. Brothers, K. N. Kudin, V. N. Staroverov, T. A. Keith, R. Kobayashi, J. Normand, K. Raghavachari, A. P. Rendell, J. C. Burant, S. S. Iyengar, J. Tomasi, M. Cossi, J. M. Millam, M. Klene, C. Adamo, R. Cammi, J. W. Ochterski, R. L. Martin, K. Morokuma, O. Farkas, J. B. Foresman and D. J. Fox, *Gaussian 16*; Gaussian, Inc.: Wallingford, CT 2016.

4 S. Watanabe, H. Nishio, T. Takayama and K. Oyaizu, *ACS Appl. Polym. Mater.*, 2023, **5**, 2307–2311.

5 S. Watanabe and K. Oyaizu, *Bull. Chem. Soc. Jpn.*, 2020, **93**, 1287–1292.